



## LETTER OPEN

Bone marrow adipopo<sup>+</sup> cell population controls bone mass via sclerostin in mice

Signal Transduction and Targeted Therapy (2023)8:265

; <https://doi.org/10.1038/s41392-023-01461-0>

## Dear editor,

The comorbidity of obesity and osteoporosis illustrates the communication and coordination of adipose and bone tissues. Leptin and adiponectin derived from adipocytes regulate osteoblast formation and function to impact bone mass through direct and indirect mechanisms.<sup>1</sup> It is known that bone marrow adipocytes (BMA) can control bone mass by modulating the bone morphogenetic protein (BMP) and other signaling pathways. BMAs can secrete soluble factors, which impact osteoblasts, osteoclasts, and osteocytes.<sup>2</sup> Sclerostin is a potent inhibitor of bone acquisition that antagonizes Wnt/ $\beta$ -catenin signaling. Deleting sclerostin was recently reported to protect against cardiovascular disease.<sup>3</sup> Furthermore, neutralizing monoclonal antibodies against sclerostin increase bone mass and are utilized to treat osteoporosis. Previous studies revealed that global ablation of sclerostin increased both trabecular and cortical bone mass<sup>4</sup> and that sclerostin produced by the osteocytes located in the bone matrix negatively regulated bone mass in mice.<sup>5</sup> However, it is not known whether sclerostin derived from other cell types also contributes to bone formation.

Hence, we have explored the contribution of adiponectin-expressing cells-derived sclerostin in control of bone mass by ablating of *Sost* gene, which encodes sclerostin, using the *Adipoq-Cre* that mainly targets adipose lineage cells. We found that mice lacking sclerostin in adiponectin-expressing cells (*Sost*<sup>*Adipoq*</sup>) had similar body weight, fat mass, and organs weight compared to their control littermates (Fig. 1a and Supplementary Fig. 1a–e). The adipocyte size of peripheral adipose tissue was not markedly impacted by *Sost* deletion (Fig. 1b). Results from the glucose tolerance test and insulin tolerance test showed that *Sost* ablation in adipopo<sup>+</sup> cells did not affect the ability to clear blood glucose (Supplementary Fig. 2a, b) and insulin sensitivity (Supplementary Fig. 2c, d). These results demonstrate that sclerostin loss in adipocytes has no marked effects on peripheral fat mass and glucose metabolism.

Results from  $\mu$ CT analyses of skeleton revealed that *Sost*<sup>*Adipoq*</sup> mice did not show marked alteration in bone mass at 1 month of age (Supplementary Fig. 3a–g). However, at 3 months of age, *Sost*<sup>*Adipoq*</sup> mice showed an increased bone mass (Supplementary Fig. 4a–f). Moreover, at the age of 5 months, bone mass of *Sost*<sup>*Adipoq*</sup> mice was significantly increased compared to control littermates, especially in female group (Fig. 1c). *Sost* deletion significantly increased the femoral bone volume/total volume, bone mineral density, trabecular number, and trabecular thickness and decreased the trabecular separation without impacting the cortical thickness (Ct.Th) (Fig. 1d, e and Supplementary Fig. 5a–d). Note: The Ct.Th was reported to be significantly increased in the global *Sost* knockout mice.<sup>4</sup> The skull size and shape were similar between the two groups (Supplementary Fig. 6a). Furthermore, the spine bone mass was not affected by *Sost* deletion (Supplementary Fig. 6b–g). Hematoxylin and eosin (H&E) staining

of the tibial sections revealed more trabecular bone in *Sost*<sup>*Adipoq*</sup> mice than in control littermates (Fig. 1f). We performed the calcein double-labeling experiments and found that the tibial bone formation was significantly accelerated in *Sost*<sup>*Adipoq*</sup> mice, as demonstrated by significant increases in the mineral apposition rate, mineralizing surface per bone surface and bone formation rate in *Sost*<sup>*Adipoq*</sup> versus control mice (Fig. 1g, h and Supplementary Fig. 7a, b). The increased bone mass in *Sost*<sup>*Adipoq*</sup> mice could be due to increased bone formation and/or decreased bone resorption. Thus, we further determined the effect of sclerostin loss on bone resorption. Tartrate-resistant acid phosphatase staining of bone sections indicated that osteoclast formation in *Sost*<sup>*Adipoq*</sup> mice was comparable to that in control littermates (Supplementary Fig. 8a, b). We further measured the serum levels of collagen type I cross-linked C-telopeptide, a biomarker for bone resorption, and observed no significant difference between the two groups (Supplementary Fig. 8c). Osterix immunofluorescence staining revealed more osteoblasts around the trabeculae in *Sost*<sup>*Adipoq*</sup> mice than in control littermates (Fig. 1i). We next examined the effect of sclerostin loss on bone mass in mice with ovariectomy (OVX). We found that *Sost* deletion ameliorated to certain extent the osteoporotic phenotypes induced by estrogen deficiency (Supplementary Fig. 9a–g).

The serum level of sclerostin protein was not significantly different between the two genotypes (Fig. 1j). Furthermore, *Sost* deletion did not change the serum levels of leptin and adiponectin, which are known to impact bone mass (Fig. 1k, l). Collectively, these results suggest the notion that it is unlikely that the high bone mass in *Sost*<sup>*Adipoq*</sup> mice is due to systemic sclerostin loss. For this reason, we next analyzed the bone marrow tissues of both genotypes. Consistent with results from peripheral fat mass analyses, perilipin staining in bone marrow was comparable, indicating that *Sost* deletion does not affect the adipocyte number and size in bone marrow tissue (Supplementary Fig. 10). We found that *Sost* inactivation promoted the formation of the bone marrow-derived colony-forming units-fibroblast (CFU-F) (Fig. 1m, n) and colony-forming units-osteoblast (CFU-OB) (Fig. 1o, p). IF staining showed that the expression level of active- $\beta$ -catenin protein was increased in KO bone compared to that in control bone (Supplementary Fig. 11). The expression levels of osteogenic marker proteins Runx2 and osterix (Osx) and alkaline phosphatase (Alp) activity, an early marker of osteogenesis, were dramatically increased in primary bone marrow stromal cell (BMSC) cultures from *Sost*<sup>*Adipoq*</sup> mice compared to those from control mice (Fig. 1q, r). Notably, the expression levels of adipogenic factors Ppar- $\gamma$  and AP2 and the adipogenic differentiation capacity of the BMSC cultures, as determined by Oil Red O staining, were not affected by *Sost* loss (Fig. 1s, t). Thus, for the first time to our knowledge, we establish that the bone marrow adipopo<sup>+</sup> cell population plays an important role in promoting BMSC osteoblast differentiation

Received: 21 November 2022 Revised: 19 April 2023 Accepted: 24 April 2023  
Published online: 10 July 2023

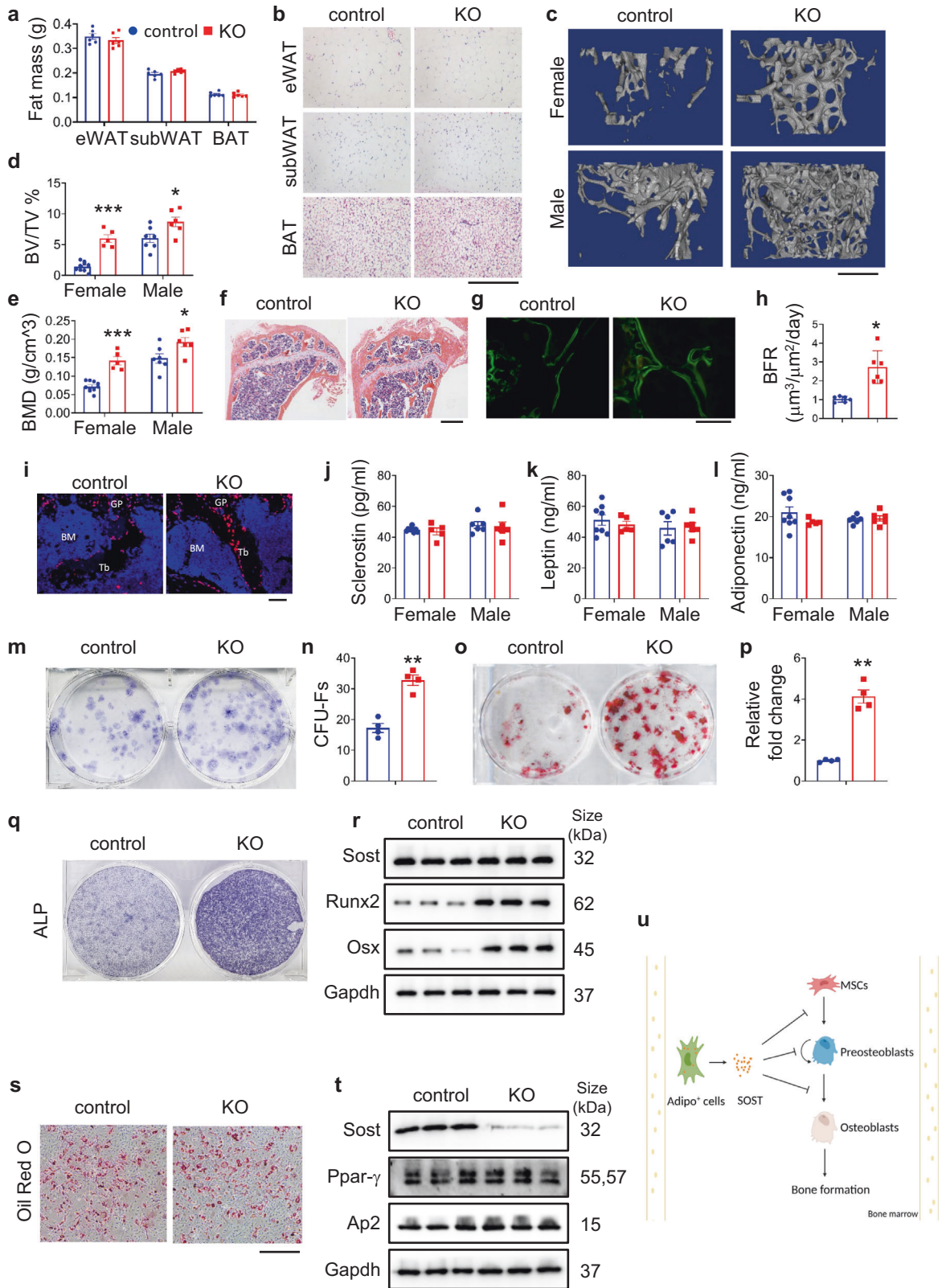


**Fig. 1** **a** Fat mass of control and KO male mice at the age of 5 months.  $N = 6$  for each group. **b** H&E staining of epididymal White Adipose Tissue (eWAT), subcutaneous White Adipose Tissue (subWAT), and Brown Adipose Tissue (BAT) of control and KO female mice fed normal chow diet for 5 months. Scale bar, 50  $\mu\text{m}$ . **c** Three-dimensional (3-D) reconstruction from micro-computerized tomography ( $\mu\text{CT}$ ) scans of distal femurs from 5-month-old control and KO mice. Scale bar, 500  $\mu\text{m}$ . Quantification of bone volume/tissue volume (**d**), bone mineral density (**e**).  $N = 10$  for female control;  $N = 5$  for female KO;  $N = 7$  for male control;  $N = 6$  for male KO. **f** H&E staining of tibial from 5-month-old female mice. Scale bar, 100  $\mu\text{m}$ . **g** Calcein double labeling staining. Representative images of 5-month-old control and KO tibial sections. Scale bar, 50  $\mu\text{m}$ . **h** Quantification of the bone formation rate of trabecular bone. **i** IF staining of osterix. Scale bar, 50  $\mu\text{m}$ . Serum levels of sclerostin (**j**), leptin (**k**) and adiponectin (**l**) from 5-month-old control and KO mice.  $N = 8$  for female control;  $N = 5$  for female KO;  $N = 6$  for male each group. **m, n** Colony forming unit-fibroblast (CFU-F) assays and quantification. **o, p** Colony forming unit-osteoblast (CFU-OB) assays and quantification. Primary BMSC was obtained from 5-month-old control and KO female mice and cultured with osteoblast differentiation medium for 7 days. Cells were used for ALP staining (**q**) and Western blot analysis with the indicated antibodies (**r**).  $N = 3$  biologically independent experiments. Primary BMSCs obtained from 5-month-old control and KO female mice were cultured with adipogenic medium for 7 days. Cells were used for Oil Red O staining (**s**) and Western blot analysis with the indicated antibodies (**t**). Scale bar, 200  $\mu\text{m}$ .  $N = 3$  biologically independent experiments. **u** A schematic illustrating how an adipog<sup>+</sup> cell population controls bone mass by producing sclerostin in the bone marrow microenvironment. Figure created using BioRender.com. \* $P < 0.05$ , \*\* $P < 0.01$ , \*\*\* $P < 0.001$  vs. controls. Results are expressed as mean  $\pm$  SEM

and bone formation (Fig. 1u). This unique cell population in the bone marrow may be a useful target for osteoporosis treatment.

#### DATA AVAILABILITY

Data are available upon reasonable request.

#### ACKNOWLEDGEMENTS

The authors acknowledge the assistance of Core Research Facilities of Southern University of Science and Technology. This work was in part supported by the National Key Research and Development Program of China Grants (2019YFA0906004), the National Natural Science Foundation of China Grants (82261160395, 82230081, 82250710175, 81991513, 82172375), the Shenzhen Municipal Science and Technology Innovation Council Grants (JCYJ20220818100617036, JCYJ20180302174246105, and ZDSYS20140509142721429) and the Guangdong Provincial Science and Technology Innovation Council Grant (2017B030301018).

#### AUTHOR CONTRIBUTIONS

Study design: G.X. and H.G. Study conduct and data collection and analysis: H.G., Y.Z., S.L., Q.Y., and X.Z. Data interpretation: G.X. and H.G. Drafting the manuscript: G.X. and H.G. G.X. and H.G. take responsibility for the integrity of the data analysis.

#### ADDITIONAL INFORMATION

**Supplementary information** The online version contains supplementary material available at <https://doi.org/10.1038/s41392-023-01461-0>.

**Competing interests:** The authors declare no competing interests.

**Ethics:** All animal experimentation was approved by the SUSTECH Animal Care and Use Committee.

Huanqing Gao<sup>1,2</sup>✉, Yiming Zhong<sup>1</sup>, Sixiong Lin<sup>1,3</sup>, Qinnan Yan<sup>1</sup>, Xuenong Zou<sup>3</sup> and Guozhi Xiao<sup>1</sup>✉

<sup>1</sup>Department of Biochemistry, School of Medicine, Guangdong Provincial Key Laboratory of Cell Microenvironment and Disease

Research, Shenzhen Key Laboratory of Cell Microenvironment, Southern University of Science and Technology, Shenzhen 518055, China; <sup>2</sup>State Key Laboratory of Genetic Engineering and School of Life Sciences, Fudan University, Shanghai 200438, China and <sup>3</sup>Guangdong Provincial Key Laboratory of Orthopedics and Traumatology, Department of Spinal Surgery, The First Affiliated Hospital of Sun Yat-sen University, Guangzhou 510080, China These authors contributed equally: Huanqing Gao, Yiming Zhong, Sixiong Lin

Correspondence: Huanqing Gao (gaohuanqing@126.com) or Guozhi Xiao (xiaogz@sustech.edu.cn)

#### REFERENCES

- Sebo, Z. L. et al. Bone marrow adiposity: basic and clinical implications. *Endocr. Rev.* **40**, 1187–1206 (2019).
- Zou, W. et al. Ablation of fat cells in adult mice induces massive bone gain. *Cell Metab.* **32**, 801–813.e806 (2020).
- Yu, Y. et al. Targeting loop3 of sclerostin preserves its cardiovascular protective action and promotes bone formation. *Nat. Commun.* **13**, 4241 (2022).
- Li, X. et al. Targeted deletion of the sclerostin gene in mice results in increased bone formation and bone strength. *J. Bone Miner. Res.* **23**, 860–869 (2008).
- Robling, A. G. & Bonewald, L. F. The osteocyte: new insights. *Annu. Rev. Physiol.* **82**, 485–506 (2020).



**Open Access** This article is licensed under a Creative Commons Attribution 4.0 International License, which permits use, sharing, adaptation, distribution and reproduction in any medium or format, as long as you give appropriate credit to the original author(s) and the source, provide a link to the Creative Commons license, and indicate if changes were made. The images or other third party material in this article are included in the article's Creative Commons license, unless indicated otherwise in a credit line to the material. If material is not included in the article's Creative Commons license and your intended use is not permitted by statutory regulation or exceeds the permitted use, you will need to obtain permission directly from the copyright holder. To view a copy of this license, visit <http://creativecommons.org/licenses/by/4.0/>.

© The Author(s) 2023